ITALIAN PHYSICAL SOCIETY

PROCEEDINGS

OF THE

INTERNATIONAL SCHOOL OF PHYSICS

«ENRICO FERMI»

COURSE CIV

edited by R. A. BROGLIA and J. R. SCHRIEFFER

Directors of the Course

VARENNA ON LAKE COMO

VILLA MONASTERO

7 - 17 July 1987

Frontiers and Borderlines in Many-Particle Physics

1988

NORTH-HOLLAND

AMSTERDAM - OXFORD - NEW YORK - TOKYO

PUBLISHED BY:

North-Holland Physics Publishing
a division of
Elsevier Science Publishers B.V.
P.O. Box 103
1000 AC Amsterdam
The Netherlands

SOLE DISTRIBUTORS FOR THE USA AND CANADA:

Elsevier Science Publishing Company Inc.
52, Vanderbilt Avenue
New York, N.Y. 10017
U.S.A.

Technical Editor
P. PAPALI

Library of Congress Cataloging-in-Publication Data

International School of Physics "Enrico Fermi" (1987 : Varenna, Italy)
Frontiers and borderlines in many-particle physics : Varenna on Lake Como, Villa Monastero, 7-17 July 1987 / edited by R.A. Broglia and J.R. Schrieffer.
p. cm. -- (Proceedings of the International School of Physics "Enrico Fermi" ; course 104)
Title on added t.p : Frontiera e confini della fisica di molte particelle.
At head of title: Italian Physical Society.
ISBN 0-444-87113-6 (U.S.)
1. Solid state physics--Congresses. 2. Many-body problem--Congresses. I. Broglia, R. A. II. Schrieffer, J. R. (John Robert), 1931- . III. Società italiana di fisica. IV. Title. V. Title. Frontiera e confini della fisica di molte particelle. VI. Series: International School of Physics "Enrico Fermi." Proceedings of the International School of Physics "Enrico Fermi" ; course 104.
QC176.A1I5568 1987
530.1'44--dc19 88-38936
CIP

Proprietà Letteraria Riservata
Printed in Italy

Collective Motion in Fermi Droplets.

G. BERTSCH

Department of Physics, Michigan State University - East Lansing, MI 48824

1. – Introduction.

These lectures will discuss the dynamics of quantum systems of fermions bound by their own interactions. The main motivation and application of the techniques I will discuss is to nuclei which exhibit a great variety of possible behavior in their response. However, the techniques are certainly quite general and applicable in other systems as well. In particular, systems of simple atoms such as alkali metal clusters exhibit a number of properties similar to those of nuclei.

The first topic I will cover is the short-time response to one-body fields. A very successful technique for dealing with this situation is mean-field theory, which I will review. The nuclear giant resonances are examples of properties of the system that are well described by mean-field theory. The one-body physics is not adequate to deal with the long-time behavior of the system, and how to treat that is the main subject of these lectures. We always begin by dividing the Hamiltonian into a mean-field part and a residual interaction. In favorable cases, the residual interaction allows us to define a collective Hamiltonian that operates on some fictitious degrees of freedom, which, however, correctly simulate the motion and response of the system. Examples of large-amplitude motions that require a collective treatment are fission, exotic radioactivity and the mixing of rotational bands. We will construct from simple models of the residual interaction the collective Hamiltonian to describe these phenomena.

At moderate excitation energy a question can be posed about the system, whether the motion becomes random or is still collective. The venerable compound-nucleus model of nuclear physics assumes that the motion in an energy eigenstate is ergodic, but it is far from clear how this can be justified from considering the properties of the residual interaction. In fact, in some systems the Hamiltonian can have substantial random character and still produce eigenstates that are localized. On a shorter time scale, we can ask what macroscopic equations are appropriate to describe the motion in var-

ious energy domains. At moderate excitation, one expects dissipation in the equations, but so far only crude attempts have been made to estimate the parameters. At the end of my lectures I will briefly consider these issues with the Hamiltonians that are developed.

2. – Single-particle motion.

The starting point of theory is the Slater determinant wave function for the many-particle system. In this section we will discuss the dynamics of individual Slater determinants, and later we will combine them together to describe the complete motion of the system. In principle one constructs Slater determinants as the stationary solutions of Hartree-Fock equations. In practice, in nuclear physics, the interaction is too strong to apply Hartree-Fock theory directly to the Hamiltonian. Instead one makes an effective interaction which at the Hartree-Fock level produces a model for the wave function that satisfies the empirical constraints on nuclear energies and densities. The effective interactions can be chosen to be convenient for calculations; density-dependent contact interactions (delta-functions) work well [1] and are commonly applied, using a parametrization scheme first proposed by SKYRME. The analogous theory in solid-state physics is known as the density functional method [2]; in treating electrons in solids the major interaction is, of course, the Coulomb, but wave function effects that are not contained in Hartree theory can be easily incorporated with a density-dependent contact interaction. We formulate the Hartree theory beginning with a Hamiltonian density that is a functional of the particle density matrix, $\varrho(r, r')$,

$$\mathscr{H} = \frac{1}{2m} \sum_i \nabla \varphi_i^* \cdot \nabla \varphi_i + \mathscr{V}[\varrho] . \tag{2.1}$$

Here $\mathscr{V}[\varrho]$ is the potential-energy density and the first term is the kinetic-energy density. We have already specialized to product wave functions to write that term as a sum over single-particle wave functions φ. The Hartree equations for φ are derived by minimizing the Hamiltonian with respect to variations in φ. Of course, we require that the variation preserve the norm of the wave function, which introduces a Lagrange multiplier ε_i into the Hartree equation,

$$H_{s.p.}\varphi_i \equiv -\frac{\nabla^2}{2m}\varphi_i + \frac{\delta \mathscr{V}}{\delta \varrho}\varphi_i = \varepsilon_i \varphi_i . \tag{2.2}$$

In this equation the single-particle potential V is the functional derivative of $\mathscr{V}$ with respect to the density matrix. I shall assume in these lectures that the Hartree wave functions and energies are known and available; I will not discuss any details in finding the solution to the equations. In general, the

Hartree theory has many solutions, differing in the nodal structure of the occupied orbits. In principle the different Hartree states are not orthogonal, but in practice the solutions to the Hartree equation have differing orbital symmetry that makes them orthogonal, or, if they have the same symmetry, the overlaps are very small. We shall treat the Hartree states as if they were orthogonal.

2·1. *External fields and the linear sum rule.* – One way to study the dynamics of a system is to find its response to an external field, and we shall adopt this approach in treating the single-particle motion. A general time-dependent external field $Q(r)\varrho(r, r)$ can be added to the Hamiltonian density. The problem to be solved is then the time dependence of the wave function that evolves from a given initial condition. The equations of motion are the time-dependent Hartree equations, which have the form

$$(H_{s.p.} + Q(r, t))\varphi_i = i\frac{\partial \varphi_i}{\partial t}. \tag{2.3}$$

The effect of the external potential on the wave function is easily found in the case that the field is applied impulsively, *i.e.* we switch the field on and off over a very short time interval. Putting this delta-function time dependence into eq. (2.3), we find that the immediate effect on the wave function is only to give the individual particles a complex phase,

$$\varphi_i(r, t = 0_+) = \exp[-iQ]\varphi_i(r, t = 0_-), \tag{2.4}$$

where now $Q(r)$ is the coefficient of the delta-function in time. In this perturbed state, the particles have an added momentum ∇Q. The kinetic energy of the particles is thus increased by the amount

$$\frac{|\nabla Q|^2}{2m}. \tag{2.5}$$

Immediately after the impulse the density of the particles is the same, so the potential energy is unaltered. Thus the total energy introduced into the system by the field is given by (2.5). If we resolve the final state into energy eigenstates, and determine their amplitude by considering the field Q as a perturbation, we obtain the energy-weighted sum rule (EWSR)

$$\sum_f \langle f|Q|i\rangle^2 (E_f - E_i) = \int \frac{|\nabla Q|^2}{2m} n(r)\, \mathrm{d}^3 r. \tag{2.6}$$

Here the initial Hartree state is labeled i and the energy eigenstates in the final state are labeled f. We also define the single-particle density $n(r) =$

$= \varrho(r, r)$. This sum rule is very important for analyzing the response of the system. Because it involves only the very-short-time behavior of the particles, it is independent of the interaction. We often use the sum rule to provide a normalization to the values of a measured or calculated operator strength $\langle i|Q|f\rangle^2$.

The particles will move with the altered momentum and the wave function changes in amplitude as well as phase. If we expand the time dependence of the solution of eq. (2.3) in a power series in time, to next order the time dependence is given by

$$\varphi_i(r, t>0) \approx \exp[-iQ] \exp[-t[H, Q]]\varphi_i(r, 0_-) \approx \tag{2.7}$$
$$\approx \exp[-iQ] \exp\left[t\frac{\nabla Q}{m}\cdot\nabla\right]\varphi_i(r, 0_-) .$$

I wrote the time dependence in an exponential rather than as an added linear term to preserve the normalization of the wave function, which imposes a condition on the second-order time dependence. Also, in going to the second line of eq. (2.7) I assumed that the Hamiltonian is completely local except for the nonrelativistic kinetic-energy operator. The ultimate effect of the derivative operator in eq. (2.7) is to shift the wave function by the distance the particles with a velocity $\nabla Q/m$ would move in a time t,

$$\varphi_i(r, t>0) \approx \exp[-iQ]\varphi_i\left(r + \frac{\nabla Q}{m}\, t,\, 0_-\right). \tag{2.8}$$

Besides the displacement of the particles, there is a change of amplitude given by the divergence of the velocity field. The impulsive potential changes the wave function by making a coordinate transformation on the arguments of the single-particle orbitals. Since all the orbitals are displaced the same way, the orthogonality is preserved. Thus, if the initial state is a normalized Slater determinant, the final state will automatically be one also. So far all of the physics has been kinematics, with the Hartree potential playing no role.

I conclude this section with a formula for the inertia associated with single-particle motion. It is first necessary to define a collective coordinate. I will take the general form of eq. (2.8), taking the coefficient of ∇Q as a collective variable ε

$$\varphi_i \sim \varphi_i(r + \varepsilon\nabla Q, 0_-) . \tag{2.9}$$

Then, if the excitation energy of the system can be expressed as a constant times $\dot{\varepsilon}^2$, the inertia is I in the relation

$$E - E_0 = \tfrac{1}{2} I\dot{\varepsilon}^2 .$$

I obtain $E - E_0$ from the EWSR, eq. (2.6), and from eq. (2.8) we see that the collective coordinate is $\varepsilon = t/m$. Then the inertia is found to be

$$I = m\int |\nabla Q|^2 n \, \mathrm{d}^3 r \,. \tag{2.10}$$

This is identical to the classical inertia of an irrotational fluid. It is the smallest possible inertia for motion with a given time rate of change of the expectation value $\langle Q \rangle$. To take a specific example, consider the quadrupole field

$$Q = z^2 - \tfrac{1}{2}x^2 - \tfrac{1}{2}y^2 \,, \qquad \nabla Q = (-x, -y, 2z) \,. \tag{2.11}$$

The inertia associated with the field is evaluted for a spherical system to be

$$I^{\mathrm{e}}_{\mathrm{s.p.}} = 2m\langle r^2 \rangle A \,, \tag{2.12}$$

where A is the number of particles in the system and $\langle r^2 \rangle$ is the mean square radius of the density distribution.

2·2. *Cubic sum rule and the diabatic frequency.* – When the next order of t is examined, we encounter restoring forces that slow down the initial motion. Formally, the wave function to the next order in time is written

$$\varphi_i(r, t > 0) \approx \exp\left[-iQ\right] \exp\left[t\frac{\nabla Q}{m}\cdot\nabla\right] \exp\left[i[H, [H, Q]]\right] \varphi_i(r, 0_-) \,. \tag{2.13}$$

If we restrict ourselves to incompressible fields, the double commutator has the form

$$\left[H, \frac{\nabla Q}{m}\cdot\nabla\right] = -\frac{\sum_{\lambda\mu}(\nabla_\mu \nabla_\lambda Q)}{m^2} \nabla_\lambda \nabla_\mu + \frac{\nabla Q}{m}\cdot\nabla V \,. \tag{2.14}$$

The second term, proportional to the gradient of the Hartree potential, contains the physics of the deceleration of the particles due to their displacement in the potential field. However, the Hamiltonian is also changing in time, and with the self-consistent potential there is an additional term at this order

$$H(t) = H(0_-) + \frac{\delta V}{\delta \varrho}\, \delta\varrho(t) \,. \tag{2.15}$$

In the limit of short-range interactions, the last term just cancels the potential term in eq. (2.14). Physically, there is no deceleration from the potential if the potential moves along with the density. The entire restoring force is then due to the first term, which we will now interpret physically.

Let us return to the example of a quadrupole field, eq. (2.11). This is the simplest kind of incompressible motion possible, a uniform shear displacement. Then the displaced wave function from eq. (2.8) is

$$\varphi_i(x(1-\varepsilon), y(1-\varepsilon), z(1+2\varepsilon)) \,. \tag{2.16}$$

This transformation is just a uniform rescaling of the three Cartesian coordinates in the original wave function. If the wave function has nodes, its kinetic energy will be changed. In eq. (2.16), we squeezed the function in the z-direction, so its nodes along that axis will be closer together and the r.m.s. momentum in that direction will be higher, making a larger kinetic energy. A good way to look at this is with the Wigner representation of the single-particle density matrix, which is the quantum generalization of phase space density. Any transformation induced by single-particle operators preserves density in phase space, so a compression in the spatial coordinate must be compensated by an expansion in the momentum coordinate.

Our quadrupole field compresses the momentum distribution in the x and y directions and expands the distribution in the z-direction. This is illustrated in fig. 1. To first order in the deformation there is no change in the total en-

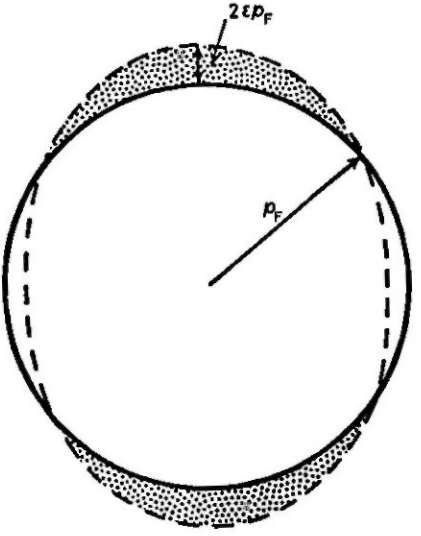

Fig. 1. – Deformation of Fermi surface associated with the scaling transformation of the wave functions, eq. (2.16).

ergy, but in second order the kinetic energy increases. We can work out what the increase is for an arbitrary deformation ε in a Fermi-gas model of the system. Because we are looking for a quantity of second order in ε, we have to make sure that the deformation preserves volume to that order. An easy

way to do this is to replace the linear scaling in eq. (2.13) by the equivalent transformation

$$x' = x \exp[-\varepsilon], \quad y' = y \exp[-\varepsilon], \quad z' = z \exp[2\varepsilon]. \tag{2.17}$$

Then the energy change per particle may be easily evaluated in the Fermi-gas model; the result is

$$\frac{\Delta E}{A} = \frac{\langle p_x^2\rangle + \langle p_y^2\rangle + \langle p_z^2\rangle}{2m} - \frac{3}{5}\frac{p_F^2}{2m} = \tag{2.18}$$

$$= \frac{p_F^2 \exp[-2\varepsilon] + p_F^2 \exp[-2\varepsilon] + p_F^2 \exp[4\varepsilon] - 3p_F^2}{10m} = \frac{6p_F^2}{5m}\varepsilon^2 + \mathcal{O}(\varepsilon^3).$$

This equation implies a very large energy cost for small changes in shape, because it is proportional to the volume of the system and to the Fermi energy. By constrast, in a liquid the deformation energy cost is only proportional to the surface area. To take a numerical example in a nuclear system, consider a heavy deformed nucleus, and let us change its deformation, increasing its semimajor axis by 1 fm. The radius is typically about 7 fm, so the deformation changes by $\Delta\varepsilon = 0.07$. For mass $A = 200$ the energy cost from eq. (2.18) is 100 MeV. This is enough excitation energy to emit a dozen nucleons and completely change the character of the nucleus.

There is a more formal way we can calculate the deformation energy. The overlap of the state created with the operator (2.14) and the state made with the commutator H and Q can be succinctly expressed in terms of a new sum rule, the cubic energy-weighted sum. This is given by

$$S_3 \equiv \sum_f \langle f|Q|i\rangle^2 (E_f - E_i)^3 = -\langle i|[H,Q][H,[H,Q]]|i\rangle. \tag{2.19}$$

This sum rule is quite useful in discussing small systems of particles, but it has also been applied to infinite systems, particularly the interacting electron gas [3, 4]. Some lengthy algebra is required to evaluate the expectation value on the right-hand side of eq. (2.20). The result for incompressible fields Q reduces to the sum of three integrals,

$$S_3 = \frac{1}{m^2}\int d^3r \sum_{\mu\nu\lambda} (\nabla_\mu \nabla_\lambda Q)(\nabla_\mu \nabla_\nu Q) \sum_i (\nabla_\lambda \varphi_i^*)(\nabla_\nu \varphi_i) + \tag{2.20}$$

$$+ \frac{1}{2m^2}\int d^3r\, \nabla\cdot(n\nabla Q)(\nabla Q)\cdot(\nabla V) + \frac{1}{2m^2}\int d^3r\, d^3r'\, \nabla\cdot(n\nabla Q)_r \frac{\delta V_{r'}}{\delta n_r}\nabla Q\cdot\nabla n_{r'}.$$

The last two terms give the effect of the potential. These terms cancel for short-range interactions. The first term in this equation involves the single-particle kinetic energy in the ground state, and when evaluated in the Fermi-

gas model is just the deformation energy of the Fermi surface that was discussed earlier.

To make the connection with eq. (2.18) more explicit, recall that the amplitude of the motion is $[H, Q]\dot{\varepsilon}$ in a time-dependent description. For a static deformation energy, we require the dependence on ε itself. If the motion is harmonic, this can be done by dividing by the frequency. We may also turn this around and define an average frequency as the ratio of sum rules,

$$\omega^2_{\rm dia} = \frac{S_3}{S_1}. \tag{2.21}$$

This is called the diabatic frequency, because it is derived from the short-time behavior of the system. This formula may also be derived by examining the high-frequency response of the system [3]. If the response is expressed as a power series in the inverse frequency, the coefficients are seen to be commutators of the Hamiltonian. Assuming the response to be dominated by a single pole, the frequency may be found from the first two terms in the power series and is identical to eq. (2.21).

If we express the sum rules in terms of the deformation-dependent energies, the ratio (2.21) is nothing more than the classical oscillator formula, the ratio of a spring constant to an inertial mass. We now have all the ingredients to determine the giant quadrupole mode of oscillation. Taking the numerator from eq. (2.18) and the denominator from eq. (2.9) and (2.12), the quadrupole frequency is given by

$$\omega^2_Q = \frac{\frac{6}{5}(p_F^2/m)\cdot A}{m\langle r^2\rangle A} = \frac{6}{5}\frac{p_F^2}{m^2\langle r^2\rangle}. \tag{2.22}$$

We see that the frequency is inversely proportional to the radius of the system. For nuclei, the predicted quadrupole frequency is at $63\ \mathrm{MeV}/A^{\frac{1}{3}}$. This value matches well with the experimental location of the giant quadrupole vibration. The observed vibration has about 75% of the EWSR, so the single-particle motion is predominant. The amplitude of the vibration can be calculated from the total energy of the excitation. If one quantum of vibration is excited, the amplitude for our heavy-nucleus example comes out to $\Delta\varepsilon = 0.025$. This is really very small, when one considers that in fission deformations with amplitudes of the order of 1 are required to go through the fission barrier.

I have also analyzed the diabatic motion of electrons in small metal particles [5]. The electrons are quite well described by mean-field theory and the same considerations apply. In this case the dominant interaction is the direct Coulomb, producing the plasmon as the collective single-particle excitation. Corrections to the classical plasmon frequency are found when one

evaluates the diabatic formula in the mean-field ground state. The formula for the plasmon ends up having the structure

$$\omega^2_{\text{dia}} = \frac{4\pi n e^2}{3m}\left(1 + \mathcal{O}\left(\frac{a}{R}\right)\right), \tag{2.23}$$

where a is the surface thickness of the electron density distribution and R is the radius of the particle. The first term is just the classical Mie frequency. The quantum corrections which mean-field theory predicts are all contained in the second term. There is no deformation energy of the Fermi surface in this case because the electrons are displaced uniformly in the Mie oscillation.

2·3. *Polarizability sum and the adiabatic frequency.* – Another important sum that I mention for completeness is the polarizability, defined by

$$\alpha = 2S_{-1} = 2\sum_i \langle i|Q|f\rangle^2 (E_f - E_i)^{-1}. \tag{2.24}$$

Because of the inverse energy weighting, this sum gives more importance to low-frequency modes, which are often the ones of greatest physical interest. One can define an average frequency of a mode using the polarizability sum along with the linear EWSR. Unfortunately, α cannot be expressed as a closed integral over the ground-state variables. To apply the sum, one must either solve the Hartree problem explicitly in an external field to polarize the system, or one must make further approximations to reduce the Hartree Hamiltonian to a classical Hamiltonian.

It is found that the shape polarizability of a Fermi droplet is very sensitive to the specific shell structures of the system. For particle numbers such that the valence shells are closed, the polarizability formula gives a result not very different from the diabatic approximation, but for open-shell systems the polarizability can be very large with transitions between low-energy single-particle states. In nuclear physics, the spin-orbit field introduces a shell structure that is rather easily distorted by a quadrupole field. What emerges is that the quadrupole strength function has a low-frequency component in addition to the giant quadrupole vibration. The amount of strength in that component is only 10% of the EWSR, but the matrix element can be very large if the frequency is low. This happens in the deformed nuclei, where the strength is concentrated in a state that is physically just part of the ground-state rotational band.

3. – Shape changes by configurational rearrangement.

We saw in sect. 2 how the single-particle field could change the shape of the system. The energy cost for Fermi systems turned out to be high, de-

pending explicitly on the Fermi energy. A more favorable way to change shape from an energetic point of view is to move particles from one orbit near the Fermi level to another. This presumes one has a residual interaction that is capable of connecting the two single-particle states. We will discuss the interaction physics in the next section; here we simply want to count states and see how much of a configurational rearrangement is necessary to achieve a given shape change. The relationship between shape and energy of configurations is shown schematically in fig. 2. The energy of different configurations is represented by the parabolic functions of deformation. As one moves

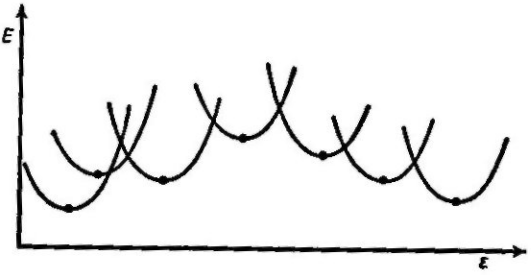

Fig. 2. – Schematic view of the energy of a fermion droplet as a function of deformation coordinate. The parabolae show the energy of individual configurations of the constrained Hartree Hamiltonian. The lowest-energy path in a large-amplitude deformation requires jumping from one Hartree configuration to another.

in shape from a given Hartree minimum, one reaches a crossing where it becomes energetically favorable to change configuration.

The counting of states can be done by making the deformation in two steps. The first step uses the single-particle field, achieving the new shape at the cost of a deformed Fermi surface. In the second step, the particles are moved between orbitals to restore the spherical Fermi surface. In the classical limit, moving particles in momentum space will not change the density distribution, as long as the volume in momentum space remains the same.

The main obstacle that can arise in carrying out this procedure is that the particle wave functions may not separate cleanly into states above and below the Fermi sphere. A given wave function might be distributed partly above and partly below the Fermi energy. Certainly in the original representation of the wave function, the transformed orbitals will straddle the surface of the Fermi sphere. However, any orthogonal transformation among the occupied orbitals has the same Slater determinant wave function, so a representation might to be found to separate particles above and below the Fermi sphere. For example, diagonalizing the single-particle Hamiltonian within the basis of the occupied orbitals would separate the single-particle state by energy. However, the difficulty of orbits straddling the Fermi level can only be overcome if there is an integral number of particles above the spherical

Fermi surface. Otherwise, moving integral numbers of particles could not restore the spherical shape. This seems to be the most important condition in practice in making a deformed state of low excitation energy.

We, therefore, deform the system enough to put an integral number of particles above the Fermi level, and then rearrange those particles. Since local density is nearly preserved on both transformations, the potential energy associated with a short-range interaction will be the same. The kinetic energy is also preserved, with the Fermi surface restored to spherical. Thus the new state will have nearly the same energy as the original state, with the changes being due to finite-range effects, and the possible imperfections in the Fermi surface with the new occupation numbers. On the average, this latter consideration would favor neither the initial nor the final state, and so would not produce any systematic error.

This procedure gives us a systematic way to change the shape of the system, keeping always to low-energy states. Let us see how this works for the quadrupole field. We first use the field to change the shape, giving a deformation ε. The new Fermi surface is now deformed by the same amount, and the number of particles above the spherical Fermi surface is given by the integral

$$(3.1)\qquad g\int_{\mathscr{V}} d^3r \int_0^{2\pi} d\varphi \frac{2}{(2\pi)^3} \int_{1/\sqrt{3}}^{1} d\cos\theta\, p_F^3\, 2\varepsilon P_2(\cos\theta) = \frac{2\varepsilon}{(2\pi)^3}\frac{4\pi}{3\sqrt{3}}\, g p_F^3 \mathscr{V} = \frac{2\varepsilon A}{\sqrt{3}}.$$

In this equation $\mathscr{V}$ is the spatial volume of the droplet and g is the degeneracy of the orbitals due to internal quantum numbers (spin and/or isospin). In the last step we expressed the phase space volume in terms of the total number of particles A in the system. The rate of configurational change as the nucleus changes shape is then given by

$$(3.2)\qquad \frac{dn}{d\varepsilon} = \frac{2A}{\sqrt{3}\, n_f},$$

where n_f is the number of particles that are moved in a given configurational change.

Equation (3.2) works quite well both for light and heavy nuclei, in cases where it has been compared to more detailed treatments of the wave function. In light nuclei, there are states at relatively low excitation known to be highly deformed, exhibiting a rotational-band structure with large quadrupole transition strengths between members of the band. According to Hartree calculations, these states are made by moving 2 protons and 2 neutrons from an orbital with a large negative quadrupole moment to one with a large positive moment. The deformations of these states are quoted in table I, comparing the empirical observed deformation with eq. (3.2). The agree-

TABLE I. – *Characteristics of deformed states in light spherical nuclei.* Equation (3.2) is applied with $n_s = 4$.

Nucleus	Deformation	
	eq. (3.2)	experimental
^{16}O	0.22	0.26
^{40}Ca	0.085	0.082

ment is surprisingly good, considering that eq. (3.2) is based on Fermi-gas arguments and the average behavior of orbitals without any specific shell effects.

It is amusing to also look at the excitation energy of these deformed states. According to the Fermi-gas picture, the kinetic energy is the same as in the ground state, and the potential energy is nearly the same for a short-range interaction. Energy differences come from liquid-drop considerations, namely the increased surface energy in the deformed state. When the energy difference is estimated by these liquid-drop considerations, it comes out in reasonable agreement with the observed excitation energy. However, this comparison is misleading because the Hartree calculations only confirm the magnitude of the deformation of these states. The energies in Hartree theory come out too high. In the theory of heavy nuclei, very detailed studies have been made of the single-particle level structure as a function of the deformation of the system [6]. One obtains level crossing schemes such as shown in fig. 3.

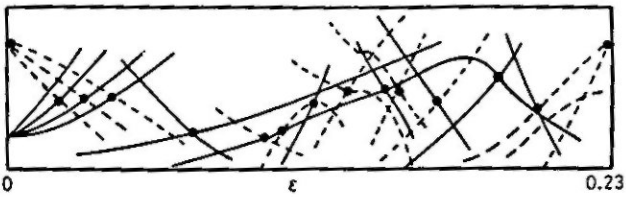

Fig. 3. – Single-particle energies of neutrons for the nucleus ^{238}U, as a function of deformation [6]. The lowest many-particle state changes configuration at the dots, which are located at the Fermi energy.

As the deformation changes, some levels dive below the Fermi energy and others emerge from the sea. Each crossing at the Fermi energy requires the particles to jump from one level to the other in order to remain in the lowest-energy state. For the interval shown in fig. 3, the total number of crossings is 29 counting both neutrons and protons. Equation (3.2) gives 32 jumps, again adding neutron jumps and proton jumps. This is a better accuracy than we know the residual interaction, and is sufficient for our purposes.

There is one other situation that I will describe in more detail later. That is the shape change that a heavy nucleus undergoes when it emits a much lighter nucleus. Such a decay in energetically allowed for heavy nuclei, but the rate is low because of the external Coulomb barrier which must be penetrated, and because there is an additional barrier penetration for the unfavored shapes. In order to describe the shape dynamics, we need to know how many configurational rearrangements are required to get from the initial nearly spherical shape to the final shape, which is that of two touching nuclei. We do this by applying a generalized version of (3.1) that includes many multipoles in the deformation field. The field is defined so that, at the end of the deformation, the multipole moments of the transformed density match the moments of the touching-sphere configuration. This is illustrated in fig. 4

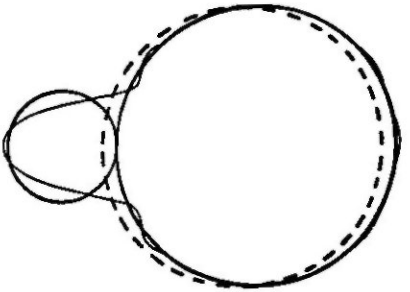

Fig. 4. – Outline of touching nuclei ^{14}C and ^{209}Pb, compared with the parent nucleus ^{223}Ra (dashed line). The shape obtained by deforming the parent distribution with an incompressible displacement field carrying multipoles up to $L = 10$ is shown with the thin line.

for the case of ^{223}Ra emitting a ^{14}C particle. In order to arrive at the final density distribution, the field must be broken down into small displacements and these applied in succession to the original density distribution. The results of this turn out to be rather simple. Namely, it is found that the number of nucleons that must jump orbit is about twice the number in the smaller of the two daughter nuclei.

It is possible to see with a simple argument the reason for correlation between the size of the daughter and the number of orbital transitions. The single-particle phase space density moves with an incompressible flow under the deformation transformations. If particles are moved out of a surface in coordinate space, then to preserve the density other particles are moved into the phase volume through a surface in momentum space. In the complete transformation, the number of particles that are moved outside the original spherical surface of the nucleus is the number in the small nucleus to be emitted, and a roughly equal number on the other side of the large nucleus to balance the center of mass at the center of the original sphere. The same

number of nucleons should be moved through the Fermi surface, and the orbital changes are required to bring them back. Later I will use this to estimate the radioactive decay rates of these nuclei.

4. – Collective motion.

4·1. *A baby model.* – Before I go into any general techniques for dealing with the configuration interactions, I will construct a very simple model that exhibits collective motion. Let us consider a linear sequence of Hartree configurations, and a residual interaction that only connects nearest-neigbor shapes, with a constant off-diagonal matrix element v. The Hamiltonian for this system is a tridiagonal matrix with elements v just off the main diagonal. It looks like this:

$$H = \begin{bmatrix} E_1 & v & 0 & \dots \\ v & E_2 & v & \dots \\ 0 & v & E_3 & \dots \\ \dots & \dots & \dots & \dots \\ \dots & \dots & \dots & \dots \\ \dots & \dots & \dots & \dots \end{bmatrix}. \tag{4.1}$$

On the main diagonal the elements are the Hartree energies of the configurations. The states are ordered in sequence according to their shapes—for example, according to increasing quadrupole moment. We want to treat the shape as a continuous degree of freedom. A connection will be obvious to anyone who has solved the one-dimensional Schrödinger equation on a mesh in coordinate space. The second derivative operator in the Hamiltonian is replaced by a second difference operator, which corresponds to a tridiagonal matrix. The same correspondence holds for the low vibrational frequencies of a linear chain of atoms. In the Hamiltonian (4.1), if the step interval between states is Δz, the kinetic-energy operator $-(\hbar^2/2I)(\partial^2/\partial z^2)$ is replaced by a matrix with

$$v = -\frac{\hbar^2}{2I\,\Delta z^2}. \tag{4.2}$$

This model of configuration mixing would be appropriate in a weak-coupling limit, where the interaction is so weak that only coupling between neigboring configurations need be considered.

In the nuclear Hamiltonian problem, the interaction is actually strong enough so that many neighboring configurations need to be treated at the same time. I will improve the model shortly, but first I want to discuss some systematic procedures for deriving collective Hamiltonians.

4·2. *Collective momenta and inertias.* – I begin assuming we have a description of the system in terms of approximate eigenstates that are labeled by some parameter. For the nuclear case, I always have in mind a parameter describing the shape of the system, for example the quadrupole moment. To make this parameter a collective coordinate one must construct a Hamiltonian that has a kinetic-energy term with a conjugate momentum. So the next task is to define momentum. Given a wave function with a smooth dependence on the coordinate, the momentum operator p may be defined in the usual way by taking the derivative of the wave function with respect to the coordinate. It is then possible to use the expectation value of p to construct states of different momentum. To be concrete, let us call the coordinate z and let $\varphi(z)$ be an approximate eigenstate at that position. For example, the state might by a constrained Hartree configuration and z the expectation value of its quadrupole moment. Then a state having momentum expectation k may be defined as follows:

$$\varphi_k^{\mathrm{sd}}(z) = \left(1 + \frac{ik}{2\langle \partial\varphi/\partial z | \partial\varphi/\partial z\rangle} \frac{\partial}{\partial z}\right)\varphi(z)\,. \tag{4.3}$$

I will call this the sudden approximation. This is only one choice of many we could make for φ_k, since the only requirement we have imposed is on the expectation value of p. For example, if the operator were part of the Hamiltonian and were turned on gradually, the components of the admixed wave function would be weighted with the reciprocal of the excitation energy, as in perturbation theory. This leads us to the adiabatic definition of the state φ_k,

$$\varphi_k^{\mathrm{ad}}(z) = \left(1 + \frac{ik}{2\langle \partial\varphi/\partial z | 1/(E-H) | \partial\varphi/\partial z\rangle} \frac{1}{E-H} \frac{\partial}{\partial z}\right)\varphi(z)\,. \tag{4.4}$$

It is rather easy to construct wave functions of this kind in Hartree theory. One simply adds to the Hartree potential a term with the momentum operator in it. For example, rotations are put into the wave function by including in the Hamiltonian a term proportional to the angular-momentum operator.

Having settled on some definition of the momentum states, we next need to see how the energy of the state depends on momentum. Then time-dependent wave packets can be constructed and the collective motion emerges directly. We simply take the expectation value of the Hamiltonian in the state (4.3) or (4.4) and see how it depends on k. Since the change in energy is second order in k, we evaluate the expectation of $H - E$ to avoid problems with the normalization in (4.3) or (4.4), that intrude at second order. Then the collective inertia I will be related to the coefficient of k^2 as

$$\langle \varphi_k | H - E | \varphi_k \rangle = \frac{k^2}{2I} + \dots\,. \tag{4.5}$$

Applying this to (4.3), we find that both the k-independent and the linear term in k vanish, leaving just a quadratic dependence, which is given by

$$\frac{1}{2I} = \frac{\langle \partial\varphi/\partial z | H - E | \partial\varphi/\partial z \rangle}{4\langle \partial\varphi/\partial z | \partial\varphi/\partial z \rangle^2} . \tag{4.6}$$

This is known as the Yoccoz inertia [7]. A different formula for the inertia may be obtained using the wave function eq. (4.4). The expectation of $H - E$ in the adiabatic state is

$$\langle \varphi_k^{\mathrm{ad}} | H - E | \varphi_k^{\mathrm{ad}} \rangle = \frac{k^2}{4} \frac{\langle \partial\varphi/\partial z | (1/(E-H))(H-E)(1/(E-H)) | \partial\varphi/\partial z \rangle}{\langle \partial\varphi/\partial z | 1/(E-H) | \partial\varphi/\partial z \rangle^2} = \tag{4.7}$$

$$= \frac{k^2}{4} \left\langle \frac{\partial\varphi}{\partial z} \middle| \frac{1}{H-E} \middle| \frac{\partial\varphi}{\partial z} \right\rangle^{-1} .$$

Then the inertia from eq. (4.5) is given by

$$I = 2 \left\langle \frac{\partial\varphi}{\partial z} \middle| \frac{1}{H-E} \middle| \frac{\partial\varphi}{\partial z} \right\rangle . \tag{4.8}$$

This treatment of the collective motion is known as the cranking model. It was first derived by including in the Hamiltonian an external time-dependent field, and relating the additional energy to the velocity of that field.

As a simple application of these techniques, let us return to the baby model defined earlier. To make a wave function that depends continuously on z, I define $\varphi(z)$ as a Gaussian wave packet of the configurations:

$$\varphi(z) \simeq \left(\frac{\alpha}{\pi}\Delta z^2\right)^{\frac{1}{4}} \sum_n \exp\left[-\alpha(z_n - z)^2/2\right] \varphi_n . \tag{4.9}$$

If α is small, the derivative wave function is given by the expression

$$\frac{\partial\varphi}{\partial z} \simeq \left(\frac{\alpha\,\Delta z^2}{\pi}\right)^{\frac{1}{4}} \sum_n \alpha(z_n - z) \exp\left[-\alpha(z_n - z)^2/2\right] \varphi_n . \tag{4.10}$$

Inserting this in eq. (4.3), we find that the state φ_k in the sudden approximation is given by

$$\varphi_k^{\mathrm{dir}} \simeq \left(\frac{\alpha\,\Delta z^2}{\pi}\right)^{\frac{1}{4}} \sum_n \left(1 + ik(z_n - z)\right) \exp\left[-\alpha(z_n - z)^2/2\right] \varphi_n . \tag{4.11}$$

This is just what we would expect from expanding a momentum factor $\exp[ikz]$.

We next evaluate the Yoccoz and adiabatic inertias. In the expression for the Yoccoz inertia, eq. (4.6), we replace the sums over n by integrals, which

is accurate if $\alpha \ll 1$. Then the expressions are equivalent to those obtained with harmonic-oscillator functions of a continuous coordinate. The resulting inertia, using the Hamiltonian (4.1), is incorrect for both the Yoccoz and adiabatic formulae. This deficiency of the Yoccoz inertia is well known, and can be rectified in various ways, such as by a momentum projection [7].

The adiabatic formula, eq. (4.8), is intended to be used with the approximate Hamiltonian that has the wave packets such as eq. (4.9) as eigenstates. Since (4.9) has the oscillator form, the approximate Hamiltonian in this case is harmonic, *i.e.*

$$H_{\text{approx}} \approx \frac{1}{2I}\left(-\frac{\partial^2}{\partial z^2} + \alpha^2 z^2\right) \tag{4.12}$$

with $I\omega = \alpha$ and $I = \frac{1}{2}(\mathrm{d}z/\mathrm{d}n)^2(1/v)$. Then the energy denominator in the adiabatic formula is ω and the expression yields the correct inertia.

The adiabatic inertia is most commonly applied with mean-field Hamiltonians. The energy denominator in the formula is then a single-particle excitation energy. An adiabatic treatment of time-dependent Hartree theory has been proposed as a way to obtain semi-quantal extensions of TDHF. References and a full discussion may be found in ref. [7].

5. – Models.

5·1. *Spin barrier model.* – In this section I will describe a model that I studied together with J. Negele, G. Puddu and P. Arve [8]. The purpose of the model is to test the various approximation methods that have been developed for treating barrier penetration in many-particle systems. The requirements of the model are first that it be simple enough so the solution can be found to whatever accuracy is desired. To test the separation between the single-particle and configurational dynamics, we include in the Hamiltonian a continuous variable, which we call z, to simulate the dependence of the single-particle wave function on position. The model also needs to have multiple Hartree minima, to mimic the physical situation when the Hartree problem is solved for fermion droplets. We accomplish this by including an additional variable in the single-particle wave function, which we treat as a spin. The two values taken by this variable then stand for two states in the transverse and other degrees of freedom. For the barrier problem, the energy of the Hartree states should be low in two regions of configuration space, separated by states of higher energy. We formulated a simple model meeting these conditions starting from a harmonic-oscillator Hamiltonian in the z coordinate for N distinguishable particles. These are coupled by two-body interaction, so additional terms are at most quadratic in the single-particle oper-

ators. The z-dependent part of our Hamiltonian is

$$H_0 = \sum_{i=1}^{N}\left(-\frac{1}{2}\frac{\mathrm{d}^2}{\mathrm{d}z^2}+\frac{1}{2}z^2\right)_i + \varkappa\left(\sum_i^N z_i\right)\left(\sum_i^N \sigma_z(i)\right). \tag{5.1}$$

The second term gives the barrier physics: the lowest-energy states have spins all up or all down, and the oscillator wells for these states are shifted to one side or the other of $z = 0$. In addition, we need to include in the Hamiltonian a part that breaks the symmetry and allows the wave function to mix with configurations in between. We take this to be a pure spin-spin interaction, specifically

$$H' = \lambda\left(\sum_i^N \sigma_z(i)\right)^2. \tag{5.2}$$

The resulting Hamiltonian may be viewed as a generalization of the Lipkin model [9] which has been used in the past for studying collective motion. The Lipkin model only has a spin coordinate, which is too simple to simulate barrier penetration with only two-body interactions. To solve the Hamiltonian by brute force, we use the eigenstates of (5.1), which may be classified according to the total azimuthal spin, $M = \langle\sum_i \sigma_z(i)\rangle$. The single-particle Hamiltonian is then just a shifted harmonic oscillator, and the orbitals are just the appropriately shifted oscillator states,

$$\varphi_\nu(z_i, M, \nu) \sim H_\nu(z + \varkappa M)\exp\left[-\tfrac{1}{2}(z+\varkappa M)^2\right]. \tag{5.3}$$

The lowest many-particle state for a given M is just the product of the ground-state orbitals. In considering excited states, note that the interaction depends only on the total spin and the total z coordinate, $Z = \sum_i z_i$. The wave function, therefore, factorizes into a part depending on Z and M, governed by the oscillator Hamiltonian, and a part that does not change. We will consider the states that couple to the lowest states, which are completely symmetric functions of the coordinates of the N particles. The internal wave function in this case is the ground-state oscillator function and the particles may as well be considered bosons. For later use I display the formulae for the matrix elements of the Hamiltonian. The shifted-oscillator representation, eq. (5.3), is used. The diagonal matrix elements are

$$\langle M, \nu|H_0 + H'|M, \nu\rangle = \frac{N}{2} + \nu - \frac{1}{2}N\varkappa^2 M^2 + \lambda N + \frac{\lambda}{2}(N^2 - M^2). \tag{5.4}$$

Here ν labels the oscillator state in the Z wave function. The off-diagonal

matrix elements connect states M with $M \pm 4$, and are given by

$$\langle M-2, \nu|H'|M+2, \nu'\rangle = \tag{5.5}$$

$$= \lambda \sqrt{\frac{N-M}{2}\frac{N+M}{2}\left(\frac{N-M}{2}+1\right)\left(\frac{N+M}{2}-1\right)}\cdot$$

$$\cdot \exp\left[-4N\varkappa^2\right](\nu'!\nu!)^{\frac{1}{2}} \sum_{n=0}^{\min(\nu',\nu)}{}' (-)^{\nu-n}\frac{1}{n!}\frac{1}{(\nu'-n)!}\frac{1}{(\nu-n)!}\left(\sqrt{\frac{N}{2}}4\varkappa\right)^{\nu'+\nu-2n}.$$

The first approximation to be considered for this Hamiltonian puts it into the framework of the baby model discussed in subsect. 4·1. This requires that we make the Hamiltonian tridiagonal. This is done by truncating to the $\nu = 0$ subspace. In effect, we throw away the single-particle degrees of freedom. It is then straightforward to derive a continuum Hamiltonian following subsect. 4·1. We choose a continuous collective coordinate x which ranges from -1 to $+1$ as M ranges from $-N$ to $+N$, *i.e.* $x = M/N$. We also drop terms of order $1/N$ to arrive at a fairly simple collective Hamiltonian

$$H_{\text{coll}} = -4|\lambda|\frac{\mathrm{d}}{\mathrm{d}x}(1-x^2)\frac{\mathrm{d}}{\mathrm{d}x} - V_0 x^2, \tag{5.6}$$

where

$$V_0 = \frac{1}{2}\varkappa^2 N^3 + \frac{\lambda - |\lambda|}{2}N^2.$$

We have used the freedom in choosing the phase of the wave function to make the relative amplitudes of different M's positive for the ground state. Hence λ appears as an absolute value in eq. (5.6). Inspecting the equation, it is obvious that the Hamiltonian has a barrier provided λ is not too negative. We call this model the continuum hopping approximation. Note that the inertia is singular near the endpoints. This is only a problem of the continuum Hamiltonian arising because terms of order $1/N$ were dropped. In sect. **6** we will compare the WKB solution of the continuum hopping model with the (numerically calculated) exact wave functions.

The next method we consider is the cranked Hartree approximation. We apply an external field in z which we use to constrain the Hartree solutions to have an given expectation value, $\langle z\rangle$. The Hartree Hamiltonian has the form

$$H_{\text{s.p.}} = -\frac{1}{2}\frac{\mathrm{d}^2}{\mathrm{d}z^2} + \frac{1}{2}z^2 + \varkappa\langle\sigma_z\rangle z + \varkappa\langle z\rangle\sigma_z + 2\lambda\langle\sigma_z\rangle\sigma_z + fz. \tag{5.7}$$

Here f is a constraining field, which is chosen to produce a solution at the desired $\langle z\rangle$. The expectation values are the matrix elements of the operators

in the many-particle Hartree state. The solution will be a single-particle wave function that has a spatial dependence exp $[-(z-\langle z\rangle/N)^2/2]$ and a spin wave function

$$\chi = \begin{pmatrix} \cos(\theta/2) \\ \sin(\theta/2) \end{pmatrix}. \tag{5.8}$$

The expectation values of the spin operators in the N-particle state are

$$\langle\sigma_z\rangle = N\cos\theta\,, \qquad \langle\sigma_x\rangle = N\sin\theta\,. \tag{5.9}$$

From the coefficients of σ_x and σ_z in the Hartree Hamiltonian we can see that the spin is oriented in the direction $(\varkappa\langle z\rangle, 2\lambda\langle\sigma_x\rangle)$. Setting this proportional to $(\langle\sigma_z\rangle, \langle\sigma_x\rangle)$, we infer that either $\langle\sigma_x\rangle = 0$ or

$$\langle\sigma_z\rangle = \frac{\varkappa\langle z\rangle}{2\lambda}. \tag{5.10}$$

These relations are sufficient to express the wave function in terms of $\langle z\rangle$.

The solution of the Hartree equations has several interesting features. First of all, all solutions have zero expectation of σ_x if the residual interaction is repulsive ($\lambda > 0$). In fact, to correspond with a physical nuclear Hamiltonian, such as one that produces a pairing ground state, the residual interaction should be attractive. So from now on, I will only discuss the case where the interaction is attractive. Then the Hartree solution may have nonzero $\langle\sigma_x\rangle$ for a limited range of $\langle z\rangle$. The locus of expectation values for the con-

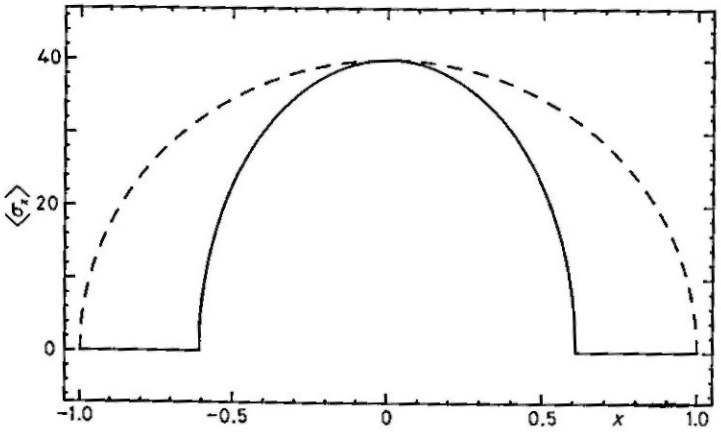

Fig. 5. – Expectation values of σ_x and $x = \langle z\rangle/\varkappa N$ for the constrained Hartree solutions to the Hamiltonian (5.1), (5.2). The solid line shows the path using the constraining field z. The dashed line uses σ_z as the constraining field. The parameters of the Hamiltonian are given in the caption to table II.

strained Hartree solutions is shown in fig. 5 for a typical parameter set. Near the endpoints of the interval, $\langle \sigma_z \rangle$ is zero and the Hartree state is the pure configuration with $M = \pm N$. The motion is entirely in the single-particle degree of freedom up to the point where the locus breaks away from the $\langle z \rangle$-axis. At that point the states of different M mix and the wave function can be continuously deformed from $M = +N$ to $M = -N$. The Hartree energies in the different regions are given by

$$E_{\text{Hartree}} = \begin{cases} \frac{N}{2} + \frac{\langle z \rangle^2}{2N} - \varkappa |\langle z \rangle| N\,, & \text{outside barrier}\,, \\ \frac{N}{2} + \frac{1}{2}\left(\frac{1}{N} + \frac{\varkappa^2}{2\lambda}\right)\langle z \rangle^2 + \lambda N^2\,, & \text{barrier region}\,. \end{cases} \tag{5.11}$$

Equation (5.11) is plotted in fig. 6 as a function of x. It may be seen that the two pieces join to make a smooth Hartree energy function. To continue the

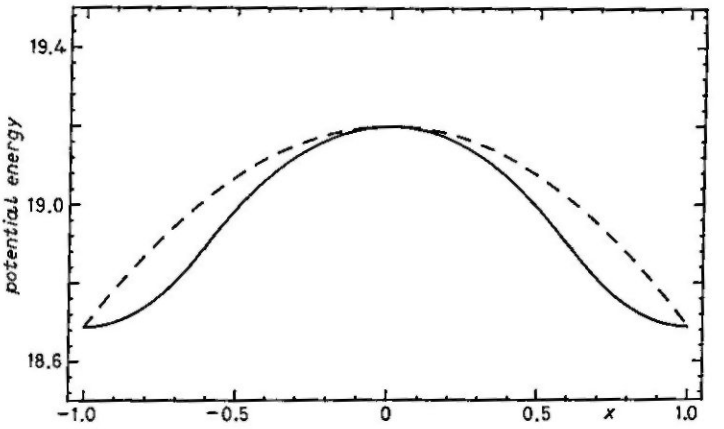

Fig. 6. – Hartree energy of the Hamiltonian (5.1), (5.2), as determined with eq. (5.11). Solid and dashed lines are for the two constrainings fields as described in the caption to fig. 5.

construction of a collective model, we apply the cranking formula, eq. (4.8), to the Hartree wave function considered as a function of $\langle z \rangle$. In the outside region the inertia just reduces to the inertia of the center-of-mass motion of N particles moving along the z axis,

$$I = 2\,\frac{|\langle \pm N, \nu = 1 | \mathrm{d}/\mathrm{d}\langle z \rangle | \pm N, \nu = 0 \rangle|^2}{E_{\nu=1} - E_{\nu=0}} = \frac{1}{N}\,. \tag{5.12}$$

There are two contributions to the inertia in the barrier region. The first is from the z-dependence of the wave function, and is identical to (5.12). There

is also a contribution from the spin dependence, and the total is

$$I = \frac{1}{N} + \frac{\varkappa^2}{8|\lambda|(4N^2\lambda^2 - \varkappa^2\langle z\rangle^2)} . \tag{5.13}$$

For the parameters we choose in the Hamiltonian, the second term dominates to the extent that the z contribution can be neglected in the inner region. Of course, it is the entire inertia outside. One last point that should be mentioned is that the inertia (5.13) becomes singular at the junction between the inner and outer regions. This is not fatal, because integrals remain well behaved, but this pathology might make cranking less reliable in this situation than with a more realistic Hamiltonian.

The final model I want to apply is the time-dependent Hartree approximation in imaginary time. This model was first developed for field theory [10] and was introduced for studying nuclear collective motion in ref. [11]. However, discussion of the details of this method is beyond the scope of these lectures.

5·2. *Pairing models.* – The Hamiltonian (5.1), (5.2) is too simplistic to exhibit many interesting aspects of pairing, such as the odd-even effects. We will now examine a Hamiltonian in which pairing is the dominant feature of the interaction and see how to construct collective dynamics. In the BCS pairing model, the interaction Hamiltonian is given by

$$H' = g \sum_{i,j}{}' a_i^\dagger a_{\bar{i}}^\dagger a_{\bar{j}} a_j , \tag{5.14}$$

where the primed sum includes the pair $(i\bar{i})$ only once. The single-particle levels are a function of the collective coordinate z, and we wish to calculate the inertia associated with motion in the z coordinate. In order to proceed, we will classify states into two types, depending on whether the single-particle energies increase or decrease with z. The many-particle wave function can be expanded in terms of states with a definite number of particles in the two categories of orbitals. Let us call n the number of pairs in the upward-moving states. Then for a fixed total number of pairs N, the wave function can be expressed as a sum over the product of wave functions of the form

$$\psi(n) = \psi_+(n)\,\psi_-(N-n) . \tag{5.15}$$

Here $\psi_\pm$ label the wave functions for the particles in the upward and downward going orbitals separately. When a pair jumps from one type of level to the other, the Hartree self-consistency is satisfied only when z changes. Thus n is a discrete coordinate that correlates with the continuous coordinate z. We can apply the continuum hopping model by calculating the interaction

matrix element between a state with one value of n and its neighbor with $n \pm 1$. The pairing matrix element connecting neighboring configurations is given by

$$(5.16)\quad v = g\langle\psi_+(n)|\sum{}' a_{\bar{i}} a_i|\psi_+(n+1)\rangle\langle\psi_-(N-n)|\sum{}' a_i^\dagger a_{\bar{i}}^\dagger|\psi_-(N-n-1)\rangle\,.$$

In the limit where $\psi_\pm$ are pure configurations the individual pair amplitudes in the above equation are 1, and we recover the weak-coupling approximation that was discussed earlier. In the presence of pairing with g larger than the single-particle level spacing, the configuration mixing enhances the pair addition and removal amplitudes in eq. (5.3). To estimate this quantitatively, we first express the pair addition amplitude in terms of the pairing gap delta using the BCS wave function

$$(5.17)\qquad \langle\psi_{\mathrm{BCS}}|\sum{}' a_i^\dagger a_{\bar{i}}^\dagger|\psi_{\mathrm{BCS}}\rangle = \frac{\Delta}{g}\,.$$

To relate this to the number-conserving states in eq. (5.2), we must establish the relationship between the BCS wave function and the number-conserving $\psi_\pm(n)$ defined above. The BCS wave function is a linear combination of these states of the form

$$(5.18)\qquad \psi_{\mathrm{BCS}} = \Big(\sum_n b_n\psi_+(n)\Big)\Big(\sum_n b_n\psi_-(N-n)\Big)\,,$$

where the b_n are amplitudes that vary smoothly with n. Assuming that the matrix elements also are smooth functions of n, the pair addition amplitude for the BCS state may be expressed in terms of the amplitudes for the $\psi_\pm$, and we find

$$(5.19)\quad \langle\psi_{\mathrm{BCS}}|\sum{}' a_i^\dagger a_{\bar{i}}^\dagger|\psi_{\mathrm{BCS}}\rangle = \sum_n b_n b_{n+1}\langle\psi_+(n+1)|\sum{}' a_i^\dagger a_{\bar{i}}^\dagger|\psi_+(n)\rangle + \\ + \sum_n b_n b_{n+1}\langle\psi_-(N-n)|\sum{}' a_i^\dagger a_{\bar{i}}^\dagger|\psi_-(N-n-1)\rangle \approx \\ \approx 2\langle\psi_\pm(n+1)|\sum{}' a_i^\dagger a_{\bar{i}}^\dagger|\psi_\pm'n)\rangle\,.$$

We now use this to evaluate matrix elements in eq. (5.16) and we arrive at a hopping matrix element

$$(5.20)\qquad v = \frac{\Delta^2}{4g}\,.$$

The resulting collective Hamiltonian is then given by

$$(5.21)\qquad H_{\mathrm{col}} = -\frac{\mathrm{d}}{\mathrm{d}z}\frac{\Delta^2}{4g}\left(\frac{\mathrm{d}z}{\mathrm{d}n}\right)^2\frac{\mathrm{d}}{\mathrm{d}z}\,, \qquad I = \frac{2g}{\Delta^2}\left(\frac{\mathrm{d}n}{\mathrm{d}z}\right)^2\,.$$

Here dz/dn is the reciprocal of the number of level crossings per unit interval of z. This quantity can be estimated by the Fermi-gas model discussed in sect. 3. Δ is known experimentally, so the only quantity that is physically obscure is the pairing interaction strength g. The relation between g and Δ involves a logarithmic cut-off on the energies included in the configuration space; nuclear models often use a cut-off of one major shell of configuration space which yields $\Delta/g \sim 5 \div 10$.

We next want to consider the cranked BCS approximation. The formula for the inertia is given by eq. (4.8). To apply it, we need to evaluate the derivative of a BCS wave function with respect to z. First let me remind you of definition of the BCS wave function. The wave function itself is the product of operators acting on the vacuum,

$$\psi = \prod_i{}' (\cos\theta_i + \sin\theta_i a_i^\dagger a_{\bar{i}}^\dagger)|\,\rangle\,. \tag{5.22}$$

The angle of mixing between the empty and occupied states is related to the pairing gap and the single-particle excitation energy $\varepsilon_i - \lambda$ by

$$\theta_i = \frac{1}{2}\,\mathrm{tg}^{-1}\frac{\Delta}{\varepsilon_i - \lambda}\,. \tag{5.23}$$

Here λ is the Fermi energy of the system. The pairing gap Δ is computed from the pairing amplitude as

$$\Delta = g\langle\psi|\sum_i a_i^\dagger a_{\bar{i}}^\dagger|\psi\rangle = g\sum_i \sin\theta_i\cos\theta_i = \frac{g\Delta}{2}\sum_i \frac{1}{\sqrt{(\varepsilon_i-\lambda)^2+\Delta^2}}\,. \tag{5.24}$$

To determine the cranking inertia, we first find the derivative of the wave function (5.22) with respect to z. On a single pair operator, the derivative is

$$\frac{\mathrm{d}}{\mathrm{d}z}(\cos\theta_i + \sin\theta_i a_i^\dagger a_{\bar{i}}^\dagger) = (-\sin\theta_i + \cos\theta_i a_i^\dagger a_{\bar{i}}^\dagger)\frac{\mathrm{d}\theta_i}{\mathrm{d}z}\,. \tag{5.25}$$

The factor in parentheses represents a normalized two-quasi-particle excitation, so the matrix element to the two-quasi-particle state is just $\mathrm{d}\varphi_i/\mathrm{d}z$. This derivative is evaluated using eq. (5.23),

$$\frac{\mathrm{d}\theta_i}{\mathrm{d}z} = \frac{-\Delta}{2\left((\varepsilon_i-\lambda)^2+\Delta^2\right)}\frac{\mathrm{d}\varepsilon_i}{\mathrm{d}z}\,. \tag{5.26}$$

The excitation energy of the two-quasi-particle state is twice the quasi-particle energy, and is given by

$$E_i - E_0 = 2e_i = 2\sqrt{(\varepsilon_i-\lambda)^2+\Delta^2}\,. \tag{5.27}$$

We collect these pieces together and insert in the formula for the cranking inertia, to find

$$I_{\mathrm{BCS}} = \frac{1}{4}\sum_i \frac{\Delta^2}{((\varepsilon_i-\lambda)^2+\Delta^2)^{\frac{3}{2}}}\left(\frac{\mathrm{d}\varepsilon_i}{\mathrm{d}z}\right)^2 . \tag{5.28}$$

An analytic estimate may now be obtained by replacing the sum over states by an integral over ε times the single-particle level density $\mathrm{d}n/\mathrm{d}\varepsilon$,

$$I_{\mathrm{BCS}} = \frac{\Delta^2}{4}\frac{\mathrm{d}n}{\mathrm{d}\varepsilon}\left(\frac{\mathrm{d}\varepsilon_i}{\mathrm{d}z}\right)^2_{\mathrm{av}}\int \frac{\mathrm{d}\varepsilon}{((\varepsilon-\lambda)^2+\Delta^2)^{\frac{3}{2}}} = \frac{1}{3\Delta^2}\left(\frac{\mathrm{d}\varepsilon}{\mathrm{d}z}\right)^2_{\mathrm{av}}\frac{\mathrm{d}n}{\mathrm{d}\varepsilon} . \tag{5.29}$$

This expression was first derived, up to an overall factor, by BRACK *et al.* [12]. It varies quadratically with the pairing gap, as we found in the hopping treatment, eq. (5.20). The two formulae for the inertia may be compared more closely if we replace $\mathrm{d}\varepsilon/\mathrm{d}z$ by a product of factors we have estimates for, $2(\mathrm{d}\varepsilon/\mathrm{d}n)(\mathrm{d}n/\mathrm{d}z)$,

$$I_{\mathrm{BCS}} = \frac{4}{3\Delta^2}\frac{\mathrm{d}\varepsilon}{\mathrm{d}n}\left(\frac{\mathrm{d}n}{\mathrm{d}z}\right)^2 . \tag{5.30}$$

We see that the two expressions eqs. (5.21) and (5.30) are not identical. In view of our experience with the baby model, we are inclined to distrust the cranking result.

Some numerical estimates are in order to make contact with the physical world. Let us consider quadrupolar inertia for a system with density n_0 and radius R. The quadrupolar coordinate will be taken as the parameter ε in the displacement field, eq. (2.9). For comparison purposes, recall the classical fluid inertia, eq. (2.12),

$$I^{\mathrm{Q}}_{\mathrm{f.d.}} = 2m\langle r^2\rangle A . \tag{5.31}$$

For a nucleus with 200 nucleons the numerical value of this inertia is $1/0.7\cdot 10^{-2}$ MeV. To compare with the hopping inertia, we apply eq. (3.2) for the level crossing rate. The pairing strength for neutrons or protons separately has the approximate value $\Delta \approx 1$ MeV. We use for g the value for the space truncation of a single major shell, $g = 0.14$ [13]. The numerical value of the inertia works out to be the following:

$$I^{\mathrm{s}} = \left(\frac{\mathrm{d}n}{\mathrm{d}z}\right)^2 \frac{2g}{\Delta_{\mathrm{n}}^2+\Delta_{\mathrm{p}}^2} = \frac{4}{3}\frac{A^2}{2^2}\frac{2(0.14)}{2} \approx \frac{1}{0.6\cdot 10^{-3}\ \mathrm{MeV}} . \tag{5.32}$$

Finally, we apply the cranked BCS formula, eq. (5.29). This requires the level density of pair states, which is related to the single-particle level den-

sity in the Fermi-gas model as follows:

$$\frac{\mathrm{d}n}{\mathrm{d}\varepsilon} = \frac{1}{2}\frac{\mathrm{d}n}{\mathrm{d}\varepsilon}\Big)_{\text{single particle}} \approx \frac{3A}{4\varepsilon_{\mathrm{F}}}. \tag{5.33}$$

The resulting inertia is then

$$I_{\mathrm{ad}} = \left(\frac{1}{\Delta_{\mathrm{n}}^2} + \frac{1}{\Delta_{\mathrm{p}}^2}\right)\frac{4}{3}\frac{4\varepsilon_{\mathrm{F}}}{3A}\frac{4A^2}{3\cdot 2^2} = \frac{8}{27}\frac{\varepsilon_{\mathrm{F}}A}{\Delta^2} \approx \frac{1}{10^{-4}\,\mathrm{MeV}}. \tag{5.34}$$

The pairing-induced inertias are similar in magnitude. They are, of course, larger than the classical inertia for small systems, which includes all observable nuclei.

What is not contained in these formulae is the approach to the classical inertia for large systems. As the size of the system is increased, the single-particle contribution becomes more important in the inertia and eventually it dominates. In order for this to happen, the energies of the single-particle excitations would have to lie in the energy gap Δ. From the estimate of the quadrupole frequency, eq. (2.22), this would only occur in nuclei containing several thousand nucleons.

6. – Findings.

In this section we apply the models discussed in sect. **5**. We first examine the results of the spin barrier model [8], which we regard as a testing ground for various approximate treatments of collective motion. The spin barrier Hamiltonian, as given by eqs. (5.4) and (5.5), can be diagonalized numerically to get « exact » results to compare with. We have to decide what parameter values to take in the Hamiltonian. The physical situation we have in mind is the spontaneous fission of nuclei, so we take $N = 40$, which is comparable to the number of orbital jumps that occur during the fission process. Also, this N is large enough so that the continuum treatment should apply. The energy scale of the single-particle Hamiltonian should be characteristic of the single-particle motion. If we identify it with the giant quadrupole frequency, then the unit of energy in the Hamiltonian (5.1) corresponds to about 10 to 15 MeV. The next parameter to be set is the physical barrier height. For the nuclear-fission problem, this has the order of magnitude of 5 MeV. Thus the parameter V_0 in eq. (5.6) should have a magnitude of $\frac{1}{3}$ to $\frac{1}{2}$. The last physical quantity is the interaction strength, which we try to set by the analogy with pairing. From the discussion at the end of sect. **5**, the empirical pairing strength connecting neighboring configurations should have a magni-

tude of about 2.5 MeV. The Hamiltonian (5.2) has a varying off-diagonal matrix element, and we have to decide whether to fit the pairing in the barrier region or outside. The middle of the barrier is the most important region, so we will pick a value of λ that gives a matrix element of about $\frac{1}{4}$ there. In the study below, we take $\lambda = -0.0005$ and $\varkappa = 0.006\,403$. This gives a matrix element between configurations of $\frac{1}{8}$ and a barrier height of 0.51.

The diagonalization of the Hamiltonian produces eigenvalues that are nearly degenerate in pairs for energies below the barrier. The splitting of the degeneracy is due to the barrier penetration. In table II we quote the en-

TABLE II. – *Eigenenergies and splitting of states for the spin barrier Hamiltonian, eqs.* (5.1), (5.2). The parameters in the Hamiltonian are $N = 40$, $\varkappa = 0.006\,403$, $\lambda = -0.000\,5$. The first two columns of splittings ΔE are the results of diagonalizing the Hamiltonian in the basis of eq. (5.3), truncating the number of oscillator quanta as indicated. The next column gives the WKB solution, eq. (6.1), using the collective Hamiltonian from the continuum hopping model, eq. (5.6). The next column gives the corresponding result from the cranked Hartree Hamiltonian, eqs. (5.12) and (5.13). Finally, the last column shows the result from the imaginary time-dependent mean-field equations.

E	$\log \Delta E$				
	diagonalization		continuum hopping	cranked Hartree	imaginary TDHF
	($\nu = 4$)	($\nu = 0$)			
0.015	– 13	– 13	– 12.4	– 19	– 13
0.170	– 8.9	– 8.9	– 9.5	– 13.8	—
0.305	– 5.9	– 5.9	– 6.1	– 6.7	—
0.418	– 3.5	– 3.5	– 3.5	– 4.2	—
0.505	– 1.9	– 1.9	– 1.7	– 1.8	—

ergies E and splittings ΔE of the low states of the Hamiltonian. Note that the degeneracy splitting becomes very small for states far below the barrier, as expected.

6·1. *Role of single-particle motion.* – The first two columns of splittings in table II show the results of the diagonalization for two truncations of the Hamiltonian. In the first case we keep oscillator states up to $\nu = 4$. Next are displayed the results keeping only $\nu = 0$ states. Comparing these two, it is clear that single-particle motion plays an insignificant role in the barrier penetration. We argued in the second section that single-particle motion was too costly from an energy point of view to be dominant, but from this result it is clear that we can neglect it completely. That conclusion depends on the

single-particle frequency being larger than the barrier height. It would be interesting to also explore what happens in the opposite limit.

The single-particle motion must also become important when a lot of energy is brought into the system through the single-particle degrees of freedom. This is the case in heavy-ion collisions at energies above the Coulomb barrier.

6·2. *Tunneling.* – We now consider the various treatments of collective tunneling and compare with the diagonalization of the spin barrier Hamiltonian. The physical quantity that can be extracted from the Hamiltonian is the splitting of the states of opposite parity with respect to the barrier top. However, the splitting depends not only on the barrier but also on the details of the wave functions in the allowed region. The number of degrees of freedom active in the allowed region will depend on the collective treatment, and the tunneling is affected because it is proportional to the wave function amplitude at the barrier. The more degrees of freedom are active in the allowed region, the smaller will be the amplitude of the wave function at the barrier and the smaller will be the splitting. So we should be careful in comparing the barrier physics of different models to treat the allowed degrees of freedom on an equal footing. The dependence of the splitting on both the barrier penetration and the allowed degrees of freedom is contained in the WKB formula for the level splitting. This is given by [14]

$$\Delta E = \frac{(\mathrm{d}n/\mathrm{d}E)^{-1}}{\pi} \exp\left[-\int p\,\mathrm{d}x\right], \tag{6.1}$$

where $\mathrm{d}n/\mathrm{d}E$ is the density of states on one side of the barrier. The exponential is the usual WKB integral for the penetration amplitude (not probability!), with limits of integration at the two classical turning points. We shall compare various treatments with the exact one using eq. (6.1), calculating the penetrability according to various collective methods. The density of states will be taken from the actual Hamiltonian,

$$\left(\frac{\mathrm{d}n}{\mathrm{d}\varepsilon}\right)_{E_i} = \frac{2}{E_{i+1} - E_{i-1}}. \tag{6.2}$$

Then splittings may be compared directly with those of the diagonalization.

Before proceeding with the comparison we make one remark on the general validity of the collective treament. Of the methods that we have applied for the tridiagonal matrix, the continuum hopping model appeared most reliable. However, there are certainly limits on the applicability of a continuum limit. The relevant parameter is the ratio of the off-diagonal matrix element, v, to the energy below the barrier. If that number is large, the amplitude of the wave function will only change by a small amount from one state to the

neighboring state. That is the condition for the validity of the collective Hamiltonian with a continuous kinetic-energy operator. The other extreme is with v small compared to the barrier height, $E_b - E$. In this case the continuum hopping model yields a wave function decaying exponentially with the dependence

$$\psi(z_n) \sim \exp\left[-\sqrt{\frac{E_b - E}{v}}\, n\right], \qquad n = \frac{z}{\Delta z}. \tag{6.3}$$

On the other hand, in this limit the wave function can be calculated by perturbation theory, which produces the expression

$$\psi(z_n) \sim \left(\frac{v}{E_b - E}\right)^n. \tag{6.4}$$

We see that the collective wave function falls off much more rapidly than does the actual wave function when $v \ll E_b - E$. Therefore, we should be suspicious of the collective approach in the far subbarrier region; tunneling rates might be larger than predicted from the collective inertias.

The results of the continuum hopping approximation for the spin barrier model are shown in table II. We see that the treatment works surprisingly well, considering the number of approximations made. Very far below the barrier, the collective tunneling falls below the actual, as expected from the above argument.

The next model we compare to is the cranked Hartree model. From table II we see that this approximation is fair for energies close to the barrier top. At low energies, the cranking model is quite poor. It is interesting to ask why the model fails. My first thought was that the adiabatic inertia is at fault. But, in fact, the inertia in eq. (5.12) is the correct inertia for particles moving along the z-axis. The trouble seems to be rather that the constrained Hartree approximation does not produce the correct path for the system to move along. We saw in fig. 5 that the path is far from smooth. To examine this point further ARVE repeated the constrained Hartree calculation using a different constraining field. He found that, if the constraining field is chosen as σ_z instead of z, the path becomes smooth—a semicircle in fact. The inertia then is nearly the same as in eq. (5.6), and the predicted splittings are much closer to the exact values.

The last technique I want to mention is the imaginary time-dependent mean-field approximation. One can derive a formula for the energy splitting between the nearly degenerate states that has an identical appearance to eq. (6.1) [15]. However, the interpretation of the prefactor $(\mathrm{d}n/\mathrm{d}E)^{-1}$ is different. The formula is only meant to be applied for the ground-state tunneling, and ω is the collective frequency of small-amplitude oscillations. This frequency is 1 in the spin barrier Hamiltonian. When the equations of the

imaginary mean-field theory are solved, it is found that the path of the tunneling is very similar to the path taken by the constrained Hartree theory, with the spin constraint rather than the spatial constraint. There are some slight differences, the most interesting being that the y component of the spin develops an imaginary expectation value. The result of the theory for ground-state tunneling is shown in the last column of table II. The method is seen to work remarkably well. Unfortunately, as presently formulated, it is only applicable to ground-state mixing.

6·3. *A physical application.* – In this subsection I will consider the physical problem of exotic radioactivity, and apply the pairing model to calculate the radioactive-decay rates. Exotic radioactivity is the emission of light nuclei such as carbon and neon nuclei from heavy parents. This phenomenon was first observed in 1984 [16], in the decay of ^{223}Ra. This nucleus normally decays by emitting an alpha-particle, but a small branch (10^{-9}) was observed for decay by emission of a ^{14}C nucleus. Exotic radioactivity is intermediate between the extremes of alpha-decay and spontaneous fission, which are both well known and have well-developed theories. The theory for alpha-decay is based on calculating a formation probability of an alpha cluster at the nuclear surface, and then calculating the penetration of the alpha-particle through the potential barrier of the daughter nucleus. The formation probability is calculated microscopically, and typically involves the ground and nearby configurations. By contrast, in the spontaneus-fission problem the barrier only exists in the many-particle shape space, and a major change in the configuration is necessary to pass through the barrier. Up to now the cranked BCS approximation has mainly been applied [12] to spontaneous fission, but the uncertainties in the potential prevent reliable calculations in any approximation.

In exotic radioactivity, there is motion below the nucleus-nucleus Coulomb barrier as well as below a shape barrier within the parent nucleus. The theoretical analysis [17] proceeds as follows. We first calculate the penetration of the external barrier, starting from a configuration of two touching daughter nuclei. The predicted decay rate is compared with the actual decay rate to get an empirical formation factor, P. These are shown in table III. Our main object is to calculate the formation factors. To do this we need the potential as well as the inertia. The potential depends on details of shell physics and would be quite involved to calculate in detail. However, we know the energy of the ground state, and from heavy-ion scattering potentials we can make a reasonable estimate of the energy of the touching nuclei. Our potential model is to connect these points with a quadratic function of the collective coordinate. The potential-energy function is shown in fig. 7. The inertia will be treated by the pair hopping model. We found in sect. 5 that the matrix elements connecting adjacent states are of the order of 2.5 MeV, and the num-

TABLE III. – *Exotic radioactivity.*

Decay	log P empirical	log P theory
^{221}Ra ^{14}C	$<-$ 7.5	– 6.9
^{222}Ra ^{14}C	– 7.7	– 7.4
^{223}Ra ^{14}C	– 8.9	– 7.2
^{224}Ra ^{14}C	– 7.1	– 7.9
^{226}Ra ^{14}C	– 7.6	– 9.0
^{231}Pa ^{24}Ne	– 14.3	– 15.7
^{232}U ^{24}Ne	– 13.5	– 15.2
^{233}U ^{24}Ne	– 15.8	– 16.4
^{241}Am ^{34}Si	$<-$ 17.6	– 17.3

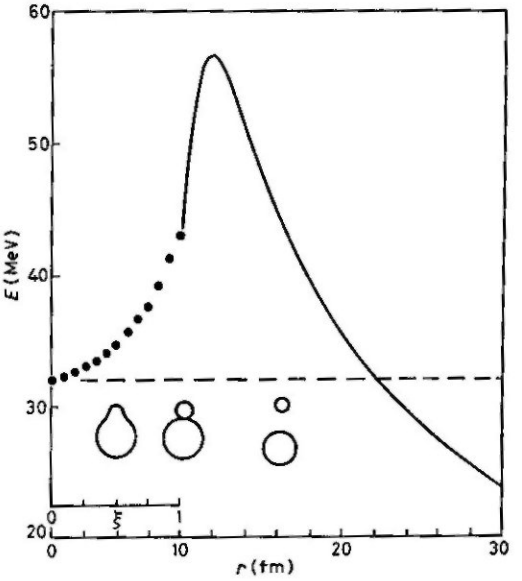

Fig. 7. – Combined barrier for exotic radioactivity. The dots indicate Hartree configurations that are connected by the residual interaction. At the point where the shape is deformed to the final daughter configuration, the barrier is the usual Coulomb barrier, modified by a short-range nuclear potential.

ber of states between the ground and the touching configuration is of the order of the number of particles in the light daughter nucleus. The continuum hopping Hamiltonian is just the harmonic oscillator, and the amplitude at the touching configuration depends on the physical quantities as

$$\psi_n \sim \exp\left[-\left(\frac{V_0}{v}n^2\right)^{\frac{1}{2}}\Big/2\right], \tag{6.5}$$

where v is the hopping matrix element, n is the number of configurations between the ground and double-sphere configuration, and V_0 is the difference in Hartree energies at these two extremes. In determining the potential, we found that the height of the potential is roughly proportional to the size of the daughter nucleus. Thus the dependence of (6.5) on the number of nucleons in the daughter comes out to be exponential, which roughly agrees with the empirical dependence. For the actual calculation, we have dropped the continuum limit and actually diagonalized the finite-dimensional hopping Hamiltonian. The results for the formation factor are shown in table III. We see rather good agreement, showing the importance of pairing in producing large-amplitude fluctuations in the ground-state shapes. The comparison of experimental and theoretical decay rates is shown in fig. 8.

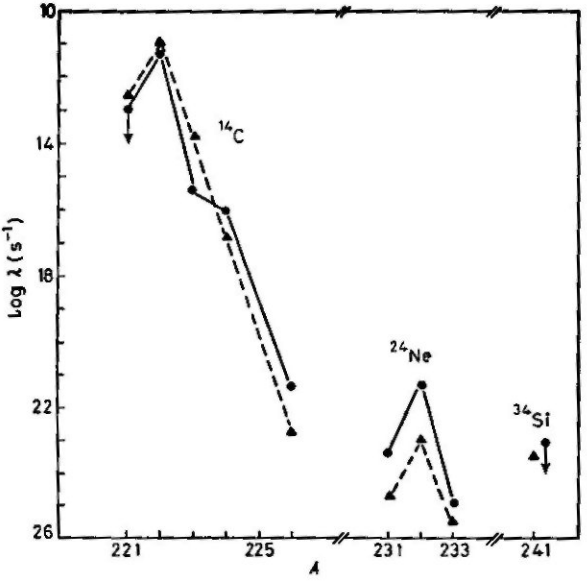

Fig. 8. – Comparison of theory and experiment for exotic radioactivity: • experiment, ▲ theory. Abscissa shows mass of parent nucleus, and ordinate is the decay rate. The experimental references are: H. Rose and G. Jones: *Nature (London)*, **307**, 245 (1984); D. Alexandrov, A. F. Beliatsky, Y. A. Gluhov, E. Y. Nikolsky, B. V. Novatsky, A. A. Ogloblin and D. N. Stepanov: *Pis'ma Ž. Éksp. Teor. Fiz.*, **40**, 152 (1984); *JETP Lett.*, **40**, 909 (1984); S. Gales, E. Hourani, M. Hussonois, J. P. Schapira, L. Stab and M. Vergnes: *Phys. Rev. Lett.*, **53**, 759 (1984); P. B. Price, J. D. Stevenson, J. D. Barwick and H. L. Ravn: *Phys. Rev. Lett.*, **54**, 297 (1985); W. Kutschera, I. Ahmad, S. G. Armato III, A. M. Friedman, J. E. Gindler, W. Henning, T. Ishii, M. Paul and K. E. Rehm: *Phys. Rev. C*, **32**, 2036 (1985); M. Paul, I. Ahmad and W. Kutschera: *Phys. Rev. C*, **34**, 1980 (1986); S. W. Barwick, P. B. Price and J. D. Stevenson: *Phys. Rev. C*, **31**, 1984 (1985); A. Sandulescu, Y. S. Zamiatnin, I. A. Lebedev, B. F. Miasoedov, S. P. Tretyskova and D. Hasegan: *JINR Rapid Commun.*, **5**, 5 (1984); S. P. Tretyakova *et al.*: *JINR Rapid Commun.*, **13**, 3 (1985).

7. – From collective to random motion.

I want to conclude my lectures touching on a topic that has many open questions, namely what happens to collective motion at finite excitation energy. Many degrees of freedom become available, and the motion can be dissipative, possibly describable with a diffusion equation. In discussing the physics here, it is common to postulate a Hamiltonian that separates into collective and noncollective coordinates, together with some coupling between them. From the point of view of Hartree theory it is not evident that one can make this separation, and I rather approach the subject by asking for the equation of motion of those degrees of freedom, such as the shape multipole moments, that exhibit collective behavior under limiting conditions. At low excitation, particularly below configurational energy barriers, we had no difficulty reducing the Hamiltonian to a tridiagonal which implies collective motion if the matrix elements are reasonably smooth. At higher excitation this truncation to tridiagonal form is no longer possible; the large number of open degrees of freedom allow motion along any particular direction to dissipate.

Let us see how this works for the pair hopping model. As before we label the states by the number of particles in the ascending orbits, n, and by α, an index to further specify the state. Also, we will restrict the state we consider to those lying within an energy interval ΔE of some definite energy. The nonzero matrix elements of the Hamiltonian are given by

$$\begin{cases} \langle n, \alpha | H | n, \alpha \rangle = E_{n\alpha}\,, & E_0 < E_{n\alpha} < E_0 + \Delta E\,, \\ \langle n+1, \alpha | H | n, \beta \rangle = v_{\alpha\beta}(n)\,. \end{cases} \tag{7.1}$$

Instead of a tridiagonal matrix, we have a band matrix with the dimension of the off-diagonal band given by the number of states in the interval ΔE.

The first observation to be made is that the off-diagonal matrix elements are very small on the scale of the collective pairing matrix elements. In the limiting situation of a Hamiltonian with all single-particle energies equal, the collective state takes all of the strength of the residual interaction and it vanishes in the noncollective states. However, in the realistic situation with an unbounded spectrum of single-particle energies there will be interaction matrix elements on the order of g for particular states. The number of states that have these matrix elements depends on the level density and the interval ΔE. Roughly, the number of states connected to a given state is

$$n = \frac{\mathrm{d}n}{\mathrm{d}\varepsilon} \Delta E\,, \tag{7.2}$$

where the level density is that of doubly occupied pair states. Suppose we truncate the space to only include these states that are coupled with matrix elements of the order of g. It is reasonable to suppose that, for any two states included, there is a unique chain of intermediate states connecting them. A Hamiltonian with this structure is known as the Bethe lattice.

In the case at hand, the energy interval over which states are strongly mixed will have the order of magnitude g. Numerically, a rough formula for g is

$$g = 25/A \text{ MeV} . \tag{7.3}$$

Using the level density formula, eq. (5.33), we find that the number of states connected is

$$n \approx \frac{3}{4} \frac{25 \text{ MeV}}{\varepsilon_F} \approx \frac{1}{2} . \tag{7.4}$$

The fact that this is less than 1 indicates that the Hamiltonian should not mix strongly, and that states should tend to be localized in configuration space. This is contrary to the elementary facts of nuclear physics that the properties of the nucleus above 5 MeV excitation are described by statistical physics—the compound-nucleus model—which requires the strong mixing of all states energetically accessible.

It is also contrary to the findings of a detailed shell model study [18]. Here the single-particle energies and residual interaction were taken from fits to the detailed spectroscopy of light nuclei ($A = 18$ to 38). We examined the eigenfunctions at very high excitation and found that they were as expected in statistical physics. Namely, the amplitudes of the different configurations in the eigenfunctions are distributed according to a Gaussian function. Obviously, the nonpairing part of the interaction is crucial for the physics at the higher excitation. We have left out the residual interaction between neutrons and protons, and this is certainly important. What is lacking is a transparent treatment of that interaction as with the pairing.

When the excitation energy is raised much higher, of the order of a hundred MeV, one passes from the domain of complete statistical physics to a domain where partial equilibration of different degrees of freedom is observed. The thermalization of the single-particle motion takes place more quickly than the equilibration in the shape degrees of freedom. This is observed by the behavior of heavy-ion reactions, which bring a large amount of energy to the coumpound system. The system can fission, but it is found to emit more neutrons before doing so than would be possible if the shape degree of freedom were equilibrated. The dynamics of this process has been described phenomenologically [19] based on Kramers [20] treatment, which uses a frictional force in the collective coordinate. What is needed is a microscopic

basis for this picture, with the dissipation and inertias derived from the physical Hamiltonian, consisting of mean fields and residual interactions.

* * *

The author acknowledges valuable discussions with R. BROGLIA, J. NEGELE, P. ARVE and U. MOSEL. The work on the spin pairing Hamiltonian was done in collaboration with J. NEGELE, P. ARVE and G. PUDDU, R. BROGLIA and B. BARRANCO collaborated on the exotic radioactivity study. The work was supported by the National Science Foundation under grant 85-19653.

REFERENCES

[1] D. VAUTHERIN and D. BRINK: *Phys. Rev. C*, **5**, 626 (1972).
[2] G. BACHELET, D. HAMANN and M. SCHLÜTER: *Phys. Rev. B*, **26**, 4199 (1982).
[3] N. IWAMOTO, E. KROTSCHECK and D. PINES: *Phys. Rev. B*, **29**, 3936 (1984).
[4] J. HOPFIELD: *Phys. Rev. B*, **2**, 973 (1970).
[5] G. BERTSCH and W. EKARDT: *Phys. Rev. B*, **32**, 7659 (1985).
[6] M. BOLSTERLI, E. FISET, J. NIX and J. NORTON: *Phys. Rev. C*, **5**, 1050 (1972).
[7] P. RING and P. SCHUCK: *The Nuclear Many-Body Problem* (Springer-Verlag, Berlin, 1980), p. 428.
[8] P. ARVE, G. BERTSCH, J. NEGELE and G. PUDDU: *Phys. Rev. C*, **36**, 2018 (1987).
[9] H. LIPKIN, N. MESHKOV and A. GLICK: *Nucl. Phys.*, **62**, 188 (1965).
[10] S. COLEMAN: *Phys. Rev. D*, **15**, 2929 (1977).
[11] S. LEVIT, J. NEGELE and Z. PALTIEL: *Phys. Rev. C*, **22**, 1979 (1980).
[12] M. BRACK, J. DAMGAARD, A. JENSEN, H. PAULI, V. STRUTINSKY and C. Y. WONG: *Rev. Mod. Phys.*, **44**, 320 (1972).
[13] A. BOHR and B. MOTTELSON: *Nuclear Structure*, Vol. II (W. A. Benjamin, New York, N. Y., 1975), eq. (6-591).
[14] L. LANDAU and E. LIFSHITZ: *Quantum Mechanics*, third edition (Pergamon Press, London, 1977), p. 183.
[15] J. NEGELE: *Rev. Mod. Phys.*, **54**, 947 (1982).
[16] H. J. ROSE and G. A. JONES: *Nature (London)*, **307**, 245 (1984).
[17] F. BARRANCO, R. BROGLIA and G. BERTSCH: *Phys. Rev. Lett.*, **60**, 507 (1988).
[18] B. A. BROWN and G. BERTSCH: *Phys. Lett. B*, **148**, 5 (1984).
[19] P. GRANGÉ, S. HASSANI, H. WEIDENMÜLLER, A. GAVRON, J. NIX and A. SIERK: *Phys. Rev. C*, **34**, 209 (1986).
[20] H. A. KRAMERS: *Physica (Utrecht)*, **7**, 284 (1940).